ORIGINAL ARTICLE
Essent Dent 2021; 1(1): 30-37
DOI: 10.5152/EssentDent.2021.21007

ISTANBUL UNIVERSITY CERRAHPASA

Computational Investigation of the Tip Effects of Various Root Canal Needles on Irrigation Performance

Selin Bulgu[1], Alperen Yıldızeli[2], Sertaç Çadırcı[2], Sema Yıldırım[1]

[1]Department of Endodontics, İstanbul University, Faculty of Dentistry, İstanbul, Turkey
[2]Department of Mechanical Engineering, İstanbul Technical University, İstanbul, Turkey

Cite this article as: Bulgu S, Yıldızeli A, Çadırcı S, Yıldırım S. Computational investigation of the tip effects of various root canal needles on irrigation performance. *Essent Dent*. *1*(1): 30-37.

Abstract

Objective: This study aimed to investigate the effects of irrigation needles with various tip shapes on the flow inside the root canal and predict their irrigation capabilities based on Computational Fluid Dynamics simulations.

Methods: Computational Fluid Dynamics simulations of 7 commonly used irrigation needle models performed, and their irrigation performances were evaluated based on apical pressure and shear stress. The working fluid representing the irrigant was water with constant thermophysical properties. Its flow was assumed to be laminar and steady at all inlet Reynolds numbers.

Results: The open-ended needles create maximum irrigant replacement toward the apex, among which the notched ones appear to be the least efficient. In contrast, the closed-ended needles show limited flow toward the apex and show lower apical pressure, which reduces the risk of apical extrusion. The apical pressure is found to be the highest for the open-ended needles with a blunt tip, followed by the open-ended, beveled needle. Lower apical pressures are observed with the GNC needle, which is a closed-ended and double side-vented irrigation needle. Among all configurations, the GNC needle outperforms others as it provides the lowest apical pressures but least irrigant penetration. On the other hand, open-ended, blunt needles showed the highest apical pressures associated with sufficient irrigant penetration.

Conclusion: The results showed that the needle tip design influences important parameters for the effectiveness and safety of the irrigation. Also, Computational Fluid Dynamics is a valuable tool in assessing the impact of needle tip designs on these parameters.

Keywords: Endodontic, Computational Fluid Dynamics (CFD), irrigation, needle, tip design

Introduction

Irrigation of root canals is considered to be essential for removing debris, bacteria, and necrotic tissues from the root canal system during chemomechanical preparation for optimal success in the root canal treatment.[1-3] About 40%-50% of the root canal wall surface remains uninstrumented owing to the complex anatomy of the root canals, and this eventually yields insufficient debridement.[4,5]

The aim of the irrigation must be irrigant penetration into the entire root canal system, and this is influenced by the irrigation needle.[6,7] Irrigation with disposable syringes and needles has been recommended as being a sufficient method.[4] Conventional syringe irrigation is considered to be the most widely used method, with the irrigant being delivered into the root canal by a syringe and needle, either passively or with agitation.[8] Irrigation needle tips are designed in various geometries to increase the efficiency of irrigation.[9,10]

Many challenges have been undertaken, and a variety of study models have been used to reach the goal of safe, effective, and predictable irrigation. These studies have attempted to describe the flow pattern of the irrigant inside the root

Corresponding Author: Selin Bulgu
dtselinbulgu@gmail.com

Content of this journal is licensed under a Creative Commons Attribution-NonCommercial 4.0 International License.

Received: May 24, 2021
Accepted: July 6, 2021
Available Online Date: August 6, 2021

canal based on macroscopic observations.[11] Yet, these studies were limited, wherein such a macroscopic approach can only provide a general description of the irrigant flow. In addition, micro-computed tomographic imaging, scanning electron microscopy, optical microscopy, root canal sectional analysis, and microbiological analysis were used to evaluate irrigation flow.[12,13] However, these methods neglect the process of fluid dynamics and only examine the final static condition.[14]

Computational Fluid Dynamics (CFD) is a numerical approach that enables finding a solution of fluid flow and heat transfer in complex geometries based on finite volume or similar methods and helps interpret and better explain the outcomes of studies.[15] Compared with conventional and experimental methods, various details of the flow can be easily obtained with CFD, especially in cases where experimental measurements are difficult to perform in a microscale flow situation.[16-20] Recent studies confirm that CFD is a powerful numerical tool to evaluate flow structures, velocity fields, shear stress, and pressure distributions in the root canal.[15,16,19,20] With its superior advantages, CFD can be considered as a promising technique to investigate the effect of needle tip design on root canal irrigation and potential irrigant extrusion risk in endodontics as in many engineering problems.

The aim of this study was to investigate the effect of various open-ended and closed-ended irrigation needles on irrigation performance and safety using CFD analysis. This was done with a simplified root canal model to assess a true root canal in a patient.

Methods

A three-dimensional model resembling a prepared root canal of a maxillary central incisor was numerically simulated. The geometry of interest consisted of the root canal and the apical part as the control volume containing two geometrical frustums of cones, as shown in Figure 1. The accepted average maxillary central incisor's length was 23.3 mm and considering geometrical simplification, the length of the root canal part was modeled as 19 mm, which is supported by Boutsioukis et al.[16] The root canal must be enlarged to 0.40 mm (ISO 40) at the apex for the irrigation to be effective, according to Ram,[21]. In correlation with this, the model has 0.45 mm apical diameter, 4% taper, and an outlet diameter of 1.21 mm. The apical part is modeled as a 0.5 mm inverted conical frustum where the narrower area is attached to the root canal tip. The apical part has a diameter of 0.3 mm at the narrower side and a diameter of 0.35 mm at the wider

Main Points

- Significant irrigant replacement is evident, the irrigant can almost reach the apex with the open-ended needles, contrary to close-ended needles that demonstrate poorer penetration of the irrigant toward the apex.
- The close-ended side-vented needles have similar shear stress distributions, maximum shear stresses are concentrated on the wall facing the outlet of the needle and the proximal outlet for the double side-vented needle types.
- The close-ended needles create much lower apical pressure compared to the open-ended needles.
- The close-ended needles have the highest averaged wall-shear stress values in the apical region.

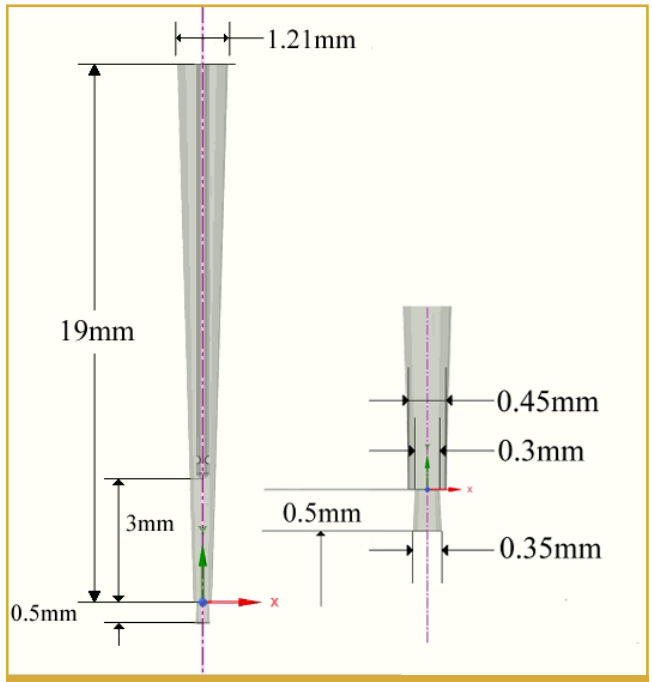

Figure 1. Dimensions of the root canal and the apical part.

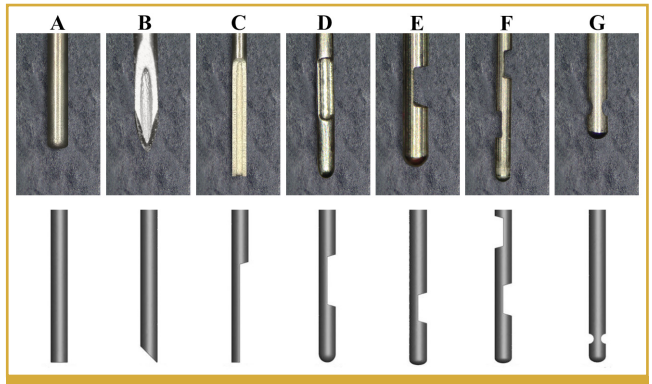

Figure 2. a-g. Commercially available irrigation needles used in this study. (a-c) Open-ended needles: (a) Open-ended needle (C-K Blunt, CK Dental, Gyeonggi-Do, Korea), (b) open-ended beveled needle (C-K Ject, CK Dental, Gyeonggi-Do, Korea), and (c) open-ended notched needle (Ultradent Endoeze, Ultradent Products Inc., South Jordan, UT, USA). (d-g) Closed-ended needles: (d) Closed-ended side-vented needle (Kerr-Hawe irrigation probe, KerrHawe SA, Biggio, Switzerland), (e) closed-ended side-vented needle (CERKAMED Endo-Top, PPH CERKAMED, Stalowa Wola, Poland), (f) closed-ended double side-vented needle (Ultradent Navitip, Ultradent Products Inc., South Jordan, UT, USA), and (g) closed-ended double side-vented needle (GNC Endo Irrigation, Tribest Dental Products, Jiangsu, China).

side. This shape conforms to the final shaping of the 45.04 AF Rotary File (Fanta Dental Material Co., Shanghai, China) used at full working length to standardize the canal shape. It should be mentioned that irrigation needles are placed 3 mm from the apex.

Seven needles that are commercially available and most widely used in clinical practice were selected, and the shape parameters of the needles were used as the basis for their 3D models (Figure 2). The two main groups of needles were identified as the closed-ended needles and the open-ended needles. The necessary information for these models has been obtained through images from a stereomicroscope (Olympus SZ61, Olympus KeyMed Comp., Tokyo, Japan). The external and internal diameters and the length of all the needles are standardized as 30 gauge (D_{ext}=320 mm, D_{int}=196 mm, and L=31 mm) in order to isolate the effect of the needle tip design on flow pattern and irrigation effectiveness.

In this study, CFD simulations of root canal irrigation flow were carried out using a finite-volume-based flow solver ANSYS Fluent 17.2. After determination of the needle configurations with appropriate boundary conditions for the accurate representation of the physical phenomenon, mesh convergence tests were performed in order to obtain mesh-independent solutions.

The problem of interest is related to the momentum transport, so the Reynolds number (Re) as given in Equation 1 below is considered to be the main dimensionless number for the problem:

$$Re = \frac{\rho V D}{\mu} \quad \text{(Equation 1)}$$

In Equation 1, V represents the average inlet velocity, D_h is the hydraulic diameter of the needle, ρ is the density, and μ is the dynamic viscosity of the fluid. The irrigant is assumed to be incompressible, homogeneous and a Newtonian fluid, e.g., distilled water, with a constant dynamic viscosity of 10^{-3} kg/m-s and a density of 1,000 kg/m^3 as standard values reported in literature.[18] Since the Reynolds number based on the hydraulic diameter of the needle is below the critical Re number (Re_{cr} = 2,300) excluding the nozzle section of the needle or needle tip, the flow is assumed to be laminar. The CFD analyzes have been carried out for a steady-state condition. The flow is single-phase, since the root canal and the needles are assumed to be completely filled with fluid.

Conservation of mass[22] in Equation (2) and laminar Navier–Stokes equations[22] in three dimensions in Equations (3–5) are solved iteratively until the convergence criteria have been achieved. The semi-implicit method for pressure-linked equations (SIMPLE) algorithm is used for pressure-velocity coupling, where a second-order upwind scheme is used for momentum equations. Convergence criteria for continuity and momentum are set to 10^{-4} and 10^{-5}, respectively.

$$\frac{\partial u}{\partial x} + \frac{\partial v}{\partial y} + \frac{\partial w}{\partial z} = 0 \quad \text{(Equation 2)}$$

$$\rho_f \left(\frac{\partial u}{\partial t} + u\frac{\partial u}{\partial x} + v\frac{\partial u}{\partial y} + w\frac{\partial u}{\partial z}\right) = -\frac{\partial p}{\partial x} + \mu\left(\frac{\partial^2 u}{\partial x^2} + \frac{\partial^2 u}{\partial y^2} + \frac{\partial^2 u}{\partial z^2}\right) \quad \text{(Equation 3)}$$

$$\rho_f \left(\frac{\partial v}{\partial t} + u\frac{\partial v}{\partial x} + v\frac{\partial v}{\partial y} + w\frac{\partial v}{\partial z}\right) = -\frac{\partial p}{\partial y} + \mu\left(\frac{\partial^2 v}{\partial x^2} + \frac{\partial^2 v}{\partial y^2} + \frac{\partial^2 v}{\partial z^2}\right) \quad \text{(Equation 4)}$$

$$\rho_f \left(\frac{\partial w}{\partial t} + u\frac{\partial w}{\partial x} + v\frac{\partial w}{\partial y} + w\frac{\partial w}{\partial z}\right) = -\frac{\partial p}{\partial z} + \mu\left(\frac{\partial^2 w}{\partial x^2} + \frac{\partial^2 w}{\partial y^2} + \frac{\partial^2 w}{\partial z^2}\right) \quad \text{(Equation 5)}$$

Boundary conditions for the problem are specified as follows:

- No-slip boundary conditions are applied on the walls of the canal and the needles,
- The apical foramen is a rigid and impermeable wall,
- Uniform velocity profile is imposed at the inlet of the needle, and
- Pressure outlet condition is defined at the outlet of the needle or needle tip.

The meshing process is performed with ANSYS Meshing, where tetrahedral and quadrilateral elements are used in the boundary regions. A representative mesh with the first needle model is shown in Figure 3.

As seen in Figure 3, to be able to capture the boundary layer flow development, dense quadrilateral elements are used in the inflation region with a growth rate of 1.3. Smaller elements are preferred in the vicinity of the canal root and the needle tip to more precisely predict velocity fields in this region.

As seen from Figure 4, mesh convergence tests are conducted to ensure that the solutions are mesh independent. Needle model D was used during mesh convergence tests. The reason behind the selection of this needle is the fact that the dimensions of needle model D are well known, and this is

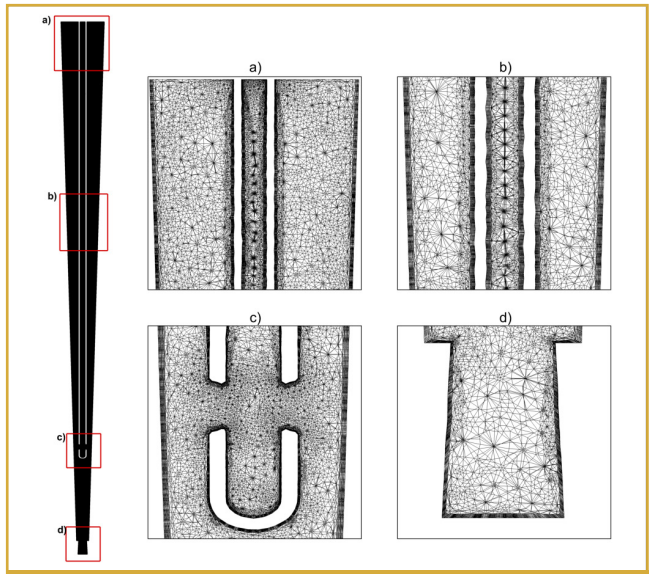

Figure 3. a–d. Representative mesh and details of different regions: (a) inlet region, (b) mid-region, (c) needle tip, and (d) apical region.

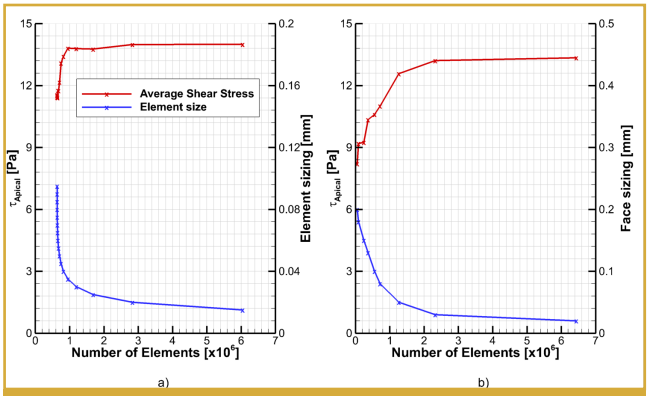

Figure 4. a, b. Mesh convergence tests: (a) element sizing and (b) face sizing.

investigated in literature as well. In this manner, mesh convergence tests are performed in two stages by changing two different parameters. The area-weighted average of apical pressure on prescribed surfaces on root and mean shear stress for all of the root is evaluated during mesh convergence tests. In the first stage, 18 different meshes with different element sizing are tested for the reference needle model. In the second stage, the effect of different face sizing on the selected evaluation parameters is considered. Consequently, a mesh consisting of approximately 2.3 million elements is found to be sufficient for further simulations.

Results

In order to understand the effect of the needle tip design, observing the flow patterns in the irrigation needles and the root canal, as well as the pressures and wall-shear stress distributions in the apex area are crucial.

Figure 5 shows the findings from the CFD simulations for 7 investigated needle geometries in terms of streamlines, velocity magnitudes, shear stress, and pressure. Streamlines indicate the route of fluid particles released from the needle inlet. They provide information on how far the irrigant can reach in the apical region; in other words, they provide information about irrigant penetration. Open-ended needles (models A, B, and C) indicate clearly different results compared with closed-ended needles (models D, E, F, and G). Significant irrigant replacement is evident; the irrigant can almost reach the apex with the open-ended needles contrary to closed-ended needles that demonstrate poorer penetration of the irrigant toward the apex. Irrigation replacement is limited to 1–1.5 mm for closed-ended needles, while extending more than 2 mm apically to the tip of open-end needles.

A dead zone is defined as the zone where the irrigant cannot penetrate. As shown in Figure 5a, among open-ended needles, models A and B show almost no dead zone, model C shows only a 1 mm dead zone, whereas almost all closed-ended needle models show a 2 mm dead zone. According to streamlines in Figure 5a, open-ended needles

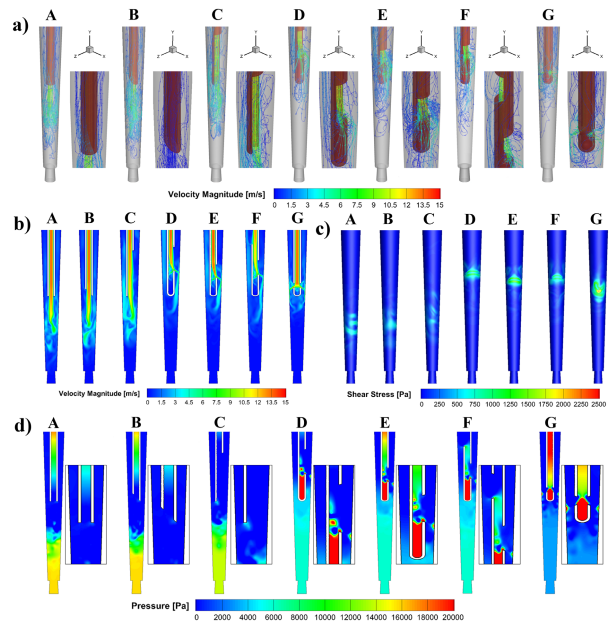

Figure 5. a-d. Computational fluid dynamics predictions for 7 irrigation needle geometries, contours of (a) streamlines, (b) velocity magnitudes, (c) shear stress, and (d) pressure.

provide strong jets directed to the apical zone and appear to break up gradually because of the irrigant present in the canal. The closed-ended, side-vented needles show an irrigant jet at the needle outlet that is first directed to the root canal wall, then toward the apex with a divergence, and finally toward the canal orifice. It should be noted that strong vortex structures predominate in the flow behavior of irrigation. For needle model F that is a closed-ended, double side-vented needle, the most intense jets are formed at the most proximal outlet, while the flow from the distal outlet presents only a minor influence on the flow structure.

Velocities above 0.1 m/s were considered clinically significant for adequate irrigant replacement.[19] As the velocity contours from Figure 5b indicate, the highest velocities are observed inside the needle lumens, and they reach a maximum value of about 12.5 m/s. As expected, the velocity profiles have the highest values at the centerline of the needle lumen, satisfying no-slip boundary conditions on the interior walls of the needle. Open-ended needle models create irrigant jets as free-shear layer flows, which are directed into the root canal in different forms depending on the needle tip design. The closed-ended needles show a sudden deceleration of the irrigant approaching the needle nozzle, and since the tip of the needle is closed, no significant irrigant penetration is observed in the apical part of the root canal.

Figure 5c shows the wall-shear stress distribution on the interior walls of the root canal. The closed-ended, side-vented needles have similar shear-stress distributions. Maximum shear stresses are concentrated on the wall facing the outlet of the needle and the proximal outlet for the double

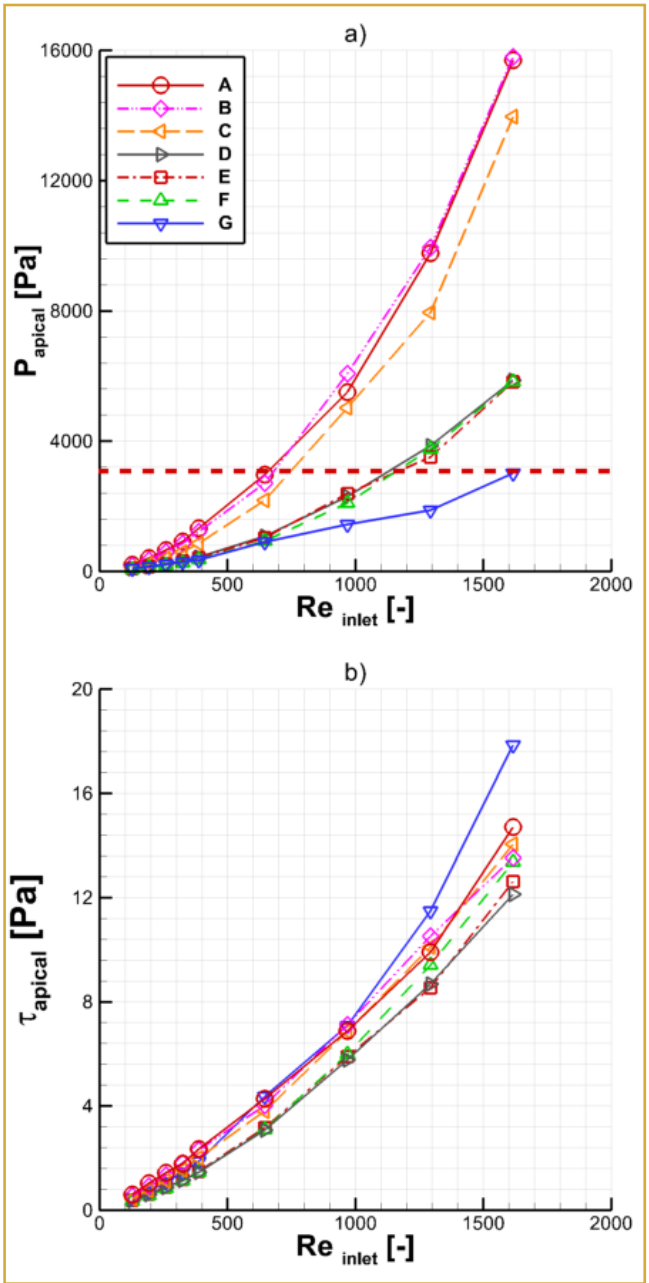

Figure 6. a, b. Computational fluid dynamics predictions for 7 irrigation needles: (a) area-weighted averaged apical pressure and (b) area-weighted averaged apical wall-shear stresses versus inlet Reynolds number.

side-vented needle types. It should be noted that the outlet velocities at the needle nozzles have a dominant effect on the wall-shear stresses.

Figure 5d demonstrates the pressure distributions in the needle lumen and the apical region. Open-ended needles create a free-shear layer flow. Thus, the irrigant jet impinges the apical region, causing stagnation pressure on the apical walls of the root canal. The pressure levels vary depending on the strength of the jet and its impingement angle. Thus, needle models A and B show the highest apical pressure, and needle model C has a comparatively lower apical pressure.

The side-vented, closed-ended needle models (D, E, F, and G) create a much lower apical pressure compared with the open-ended needles. In fact, the irrigant jet impinges the closed-ended wall of the needle, causing considerably high stagnation pressures within the needle lumen tip. For instance, needle model G offers the lowest apical pressure among all.

Figure 6 summarizes the CFD results based on area-weighted averaged apical pressure and area-weighted averaged apical wall-shear stresses at various inlet Reynolds numbers. As it can be seen from Figure 6a and has been confirmed by the pressure contours in Figure 5d, open-ended irrigation needles provide the considerably high apical pressures at all irrigant flow rates, i.e., inlet Reynolds numbers. If clinically tested threshold value for apical pressure is assumed not to exceed 3,000 Pa, closed-ended needles should be the safer choice, since they perform well in a wide range of operating flow rates. Commercially available open-ended irrigation needles should only be regarded if the irrigation is performed at low flow rates corresponding to maximum inlet Reynolds numbers 600.

Figure 6b shows the area-weighted, averaged apical wall-shear stresses at various inlet Reynolds numbers. Contrary to apical pressure, closed-ended irrigation needles have the highest averaged wall-shear stress values in the apical region. However, all needle types show similar wall-shear stresses with significant deviations only at high flow rates.

Discussion

In studies about the effectiveness of irrigation, parameters such as the geometry of the root canal; volume, pressure, and flow rate of the irrigant; and the type, size, and insertion depth of the irrigation needle have been examined.[10,20] This paper represents our first attempt to apply CFD to the investigation of the root canal irrigation. The purpose of this study is to monitor the effect of different irrigation needle geometries on irrigant flow and compare their performances.

There are several different types of irrigation needles on the market, and the main objectives of various designs are to maximize the effectiveness and safety of irrigation.[4,23] It has been reported that the use of small-diameter needles leads to more efficient irrigant replacement than larger-diameter needles,[6,24] and they may therefore result in better debridement.[24,25] In our study, 30-gauge needles were used because, according to Shen et al.[9], they are small enough to allow for irrigant exchange without forceful apical extraction.[23]

The root canal should be flushed with an irrigant while the irrigation needle tip is placed in the apical third of the root canal during preparation, according to Zehnder.[11] In the large root canals, the irrigant had approached to the apex when the needle tips were placed close to the apex[14,21]. On the

other hand, open-ended irrigation needles should not be placed at 1 mm from the apex because of high apical pressure.[17] Needle tips have been inserted at various depths in a root canal (3–6 mm short of the working length [WL])[14,16,19] Also, Shen et al.[9] showed that the irrigant either completely reached or almost reached the apex when the needles were placed 3 mm short of the WL. Complementary to them, in our study, the needles were positioned at 3 mm short of the WL.

Sodium hypochlorite solutions are widely recommended in clinical endodontic practice, [11,23] and distilled water has close density and dynamic viscosity to that of sodium hypochlorite.[26] Hence, sodium hypochlorite and water exhibit the same flow characteristics. In our study, water was used as the irrigant. The simulated root canal was assumed to be completely filled with the irrigant in all cases in order to simplify the CFD model. There is a possibility of air bubble entrapment in the most apical part of the root canal during irrigation. However, the extent of air bubble entrapment was very limited and could be ignored. This finding is actually supported by Gulabivala et al.[27] and Adıgüzel et al.[28] Therefore, the influence of bubble entrapment was neglected in the simulations reported in this study.

No-slip boundary conditions were applied on the walls of the needles and the canal root. It was assumed that both the root canal walls and those of the needle were stationary, smooth walls. The apical foramen was simulated as an impermeable and rigid wall because of existing limitations of the applied model. As long as the flow remains laminar, wall roughness was expected to have a limited effect on pressure drop.[29] Simulating the apical foramen as an impermeable wall does not exclude the possibility of irrigant extrusion toward the periapical tissue, and the evaluation of irrigant pressure applied at this impermeable wall can give information about the possibility and severity of irrigant extrusion.[30]

Irrigant velocity and dynamics on the root canal wall have a significant role in debris removal, tissue dissolution, and antimicrobial effectiveness.[9] The pressure difference developed between the syringe barrel and the root canal is the cause of irrigant flow and determines the flow rate. The flow rate of the irrigant has a significant effect on irrigant replacement throughout the canal, but it does not directly affect flow pattern within the root canal.[15] In all cases, stagnant behavior of the irrigant has been seen within the most apical part of the root canal. Minimum irrigant replacement was observed in the closed-ended models (D-G) through CFD analysis. Irrigant replacement that apically extended to the needle tip was 2.5 mm for models A and B, 2 mm for model C, 1.5 mm for models D, E, and F, and 1 mm for model G, as shown in Figure 5.

In this study, laminar flow conditions were ensured by calculating the inlet Reynolds number, which was below 2,300 for all the cases and consistent with the data given in the literature from Boutsioukis et al. and Adıgüzel et al.[17,19,28] While the irrigant flow was laminar, the streamlines were not as smooth as expected. Slow replacement cannot be considered adequate, and velocities higher than 0.1 m/s should be considered clinically significant for adequate irrigant replacement.[19]

Wall-shear stress has an impact on the detachment of debris and is directly associated with the efficacy of the irrigation. Although quantitative data on the required minimum shear stress do not exist, the distribution of the shear stress along the root canal wall provides us the evidence about the debridement efficacy of each needle type. Unfortunately, detachment of the biofilm or debris cannot guarantee their removal from the root canal, unless there is a favorable irrigant flow to carry them toward the canal orifice.[19,28] The area of high shear stress was identified in the apical part of the canal and quite close to the tip of the needle in this study (Figure 5c), which is in agreement with Boutsioukis et al.[19] The wall-shear stress was higher when the closed-ended, side-vented needle models (D-G) were used, and it was the highest for model G, which has the smallest side vent.

Irrigant extrusion toward the periapical area is known to occur in clinical practice. Irrigant extrusion has been associated with forceful delivery of the irrigant. When the tissue back pressure is overcome by irrigant pressure, there is a possibility of irrigant extrusion, and it is more likely to occur with the presence of periapical lesions.[6,7,21] It is strongly recommended that any needle lies passively in the canal and does not penetrate the walls, as the needle binding to the canal wall will likely result in the blockage of backflow and forced extrusion of the irrigant into the periapical tissue. There is no definite evidence on the minimum irrigant pressure that leads to extrusion, so there are no safety limits set for the apical wall pressure.[9,17] Guyton et al.[31] measured interstitial tissue pressure, and it ranged from 2,666 to 3,999 Pa (20–30 mmHg), mean value 3,333 Pa (25 mmHg). Also, pathological conditions can reduce interstitial tissue pressure to 1,333 Pa (10 mmHg). Therefore, the mean value of the interstitial tissue pressure may represent the limit at which periapical extruding is possible, and this assumption is supported by Salzgeber et al.,[7] who found increased apical irrigant extrusion in cases of root canals containing necrotic pulp tissue versus cases of root canals with vital pulp tissue.

In this study, we did not see any significant advantage of models B and C over model A, and for the models B and C, the flow velocity was slightly higher at the exits because of the beveled and notched needle tips (Figure 5b). Moreover, the sharp tip of the beveled needle might increase the risk of needle wedging inside the root canal, and it also possesses serious risks of injury for both the patient and the dentist, as mentioned by Boutsioukis et al.[19]

It has been reported that the side-vented, closed-ended needles are more efficient than the beveled and notched ones in the removal of a dye or bioluminescent bacteria.[10] This study did not investigate the detachment of debris or microbes from the canal wall to assess the ability of needles.

It rather investigated the exchange of the dye particles and the bioluminescent bacteria in the irrigant. Their results contradict with the current findings; side-vented, closed-ended needles have higher shear stress on the canal wall. They also have lower apical pressure and irrigant exchange that is limited and lower than those with beveled and notched ones. In addition, the flow on the side opposite to the vent was very low (Figure 5). These results are in line with earlier studies that also reported limited irrigant exchange for the side-vented needle.[9,11,16]

A lower apical wall pressure might have a negative impact on the effectiveness of irrigation in some areas of the canal, but it indicates improved safety. The results indicated that the closed-ended needles have a lower apical pressure, whereas open-ended needles have higher apical pressure, which is consistent with other studies.[9,19] The lower apical pressure supports the claims of a reduced risk of apical extrusion for closed-end endodontic needles available on the market.

In this study, it was confirmed that the shear stresses developed by models D, E, F, and G were significantly higher on the wall facing the needle vent. For the double side-vented needles, the proximal outlet mostly affected the overall performance and the outlet that was further from the apical did not seem to provide any advantage, which was in agreement with previous studies.[10,19] An additional disadvantage for all needle types was the concentration of high shear stress on a very limited area.

Needle model G appeared to be safer than other models in terms of apical extrusion. On the other hand, the limited penetration and replacement of the irrigant apically necessitates needle placement very close to the apex in the root canal. Specifically, needle model G can be recommended since it satisfies apical extrusion condition at all operating conditions. In this respect, closed-end needles are considered to be safer than open-ended needles in terms of irrigant extrusion toward the periapical tissue, and needle model G can be suggested as the safest among all the models.

In conclusion, the findings in this paper can lead to the determination of factors that can enhance or lessen the root canal treatment. The results showed that needle tip design influences important parameters for the effectiveness and safety of the irrigation. In addition, CFD is a valuable tool for assessing the impact of needle tip designs on these parameters. The CFD results of the investigated irrigation models were clinically realistic and within the limitations of the current study design.

Ethics Committee Approval: Ethics committee was not taken because there were no volunteer patients and real teeth were not used in our study.

Informed Consent: N/A.

Peer-review: Externally peer-reviewed.

Author Contributions: Concept – S.B., A.Y., S.Ç.; Design – S.B., A.Y., S.Ç.; Supervision – S.Ç., S.Y.; Resources – S.B., S.Ç.; Materials – S.B., A.Y., S.Ç.; Data Collection and/or Processing – S.B., A.Y., S.Ç.; Analysis and/or Interpretation – S.B., A.Y., S.Ç.; Literature Search – S.B.; Writing Manuscript – S.B., A.Y., S.Ç.; Critical Review – S.B., A.Y., S.Ç., S.Y.; Other – S.B., A.Y., S.Ç., S.Y.

Conflict of Interest: The authors have no conflicts of interest to declare.

Financial Disclosure: The authors declared that this study has received no financial support.

References

1. Haapasalo M, Endal U, Zandi H, Coil JM. Eradication of endodontic infection by instrumentation and irrigation solutions. *Endodontic Topics*. 2005;10(1):77-102. [Crossref]
2. Lee SJ, Wu MK, Wesselink PR. The effectiveness of syringe irrigation and ultrasonics to remove debris from simulated irregularities within prepared root canal walls. *Int Endod J*. 2004;37(10):672-678. [Crossref]
3. Gulabivala K, Patel B, Evans G, Ng Y-L. Effects of mechanical and chemical procedures on root canal surfaces. *Endodontic Topics*. 2005;10(1):103-122. [Crossref]
4. Peters OA. Current challenges and concepts in the preparation of root canal systems: a review. *J Endod*. 2004;30(8):559-567. [Crossref]
5. Peters OA, Laib A, Gohring TN, Barbakow F. Changes in root canal geometry after preparation assessed by high-resolution computed tomography. *J Endod*. 2001;27(1):1-6. [Crossref]
6. Druttman AC, Stock CJ. An in vitro comparison of ultrasonic and conventional methods of irrigant replacement. *Int Endod J*. 1989;22(4):174-178. [Crossref]
7. Salzgeber RM, Brilliant JD. An in vivo evaluation of the penetration of an irrigating solution in root canals. *J Endod*. 1977;3(10):394-398. [Crossref]
8. Dutner J, Mines P, Anderson A. Irrigation trends among American Association of Endodontists members: a web-based survey. *J Endod*. 2012;38(1):37-40. [Crossref]
9. Shen Y, Gao Y, Qian W, et al. Three-dimensional numeric simulation of root canal irrigant flow with different irrigation needles. *J Endod*. 2010;36(5):884-889. [Crossref]
10. Vinothkumar TS, Kavitha S, Lakshminarayanan L, Gomathi NS, Kumar V. Influence of irrigating needle-tip designs in removing bacteria inoculated into instrumented root canals measured using single-tube luminometer. *J Endod*. 2007;33(6):746-748. [Crossref]
11. Zehnder M. Root canal irrigants. *J Endod*. 2006;32(5):389-398. [Crossref]
12. Hockett JL, Dommisch JK, Johnson JD, Cohenca N. Antimicrobial efficacy of two irrigation techniques in tapered and nontapered canal preparations: an in vitro study. *J Endod*. 2008;34(11):1374-1377. [Crossref]
13. Nielsen BA, Craig Baumgartner J. Comparison of the EndoVac system to needle irrigation of root canals. *J Endod*. 2007;33(5):611-615. [Crossref]
14. Hsieh YD, Gau CH, Kung Wu SF, Shen EC, Hsu PW, Fu E. Dynamic recording of irrigating fluid distribution in root canals using thermal image analysis. *Int Endod J*. 2007;40(1):11-7. [Crossref]
15. Tilton J. Fluid and particle dynamics. In: Perry RH, Green DW, Maloney JO, eds. Perry's chemical engineers' handbook. 7th ed. McGraw-Hill; 1999:1-50.
16. Boutsioukis C, Lambrianidis T, Kastrinakis E. Irrigant flow within a prepared root canal using various flow rates: a Computational Fluid Dynamics study. *Int Endod J*. 2009;42(2):144-155. [Crossref]
17. Boutsioukis C, Lambrianidis T, Verhaagen B, et al. The effect of needle-insertion depth on the irrigant flow in the root canal:

evaluation using an unsteady computational fluid dynamics model. *J Endod*. 2010;36(10):1664-1668. [Crossref]
18. Boutsioukis C, Verhaagen B, Versluis M, Kastrinakis E, van der Sluis LW. Irrigant flow in the root canal: experimental validation of an unsteady Computational Fluid Dynamics model using high-speed imaging. *Int Endod J*. 2010;43(5):393-403. [Crossref]
19. Boutsioukis C, Verhaagen B, Versluis M, Kastrinakis E, Wesselink PR, van der Sluis LW. Evaluation of irrigant flow in the root canal using different needle types by an unsteady computational fluid dynamics model. *J Endod*. 2010;36(5):875-879. [Crossref]
20. Gao Y, Haapasalo M, Shen Y, et al. Development and validation of a three-dimensional computational fluid dynamics model of root canal irrigation. *J Endod*. 2009;35(9):1282-1287. [Crossref]
21. Ram Z. Effectiveness of root canal irrigation. *Oral Surg Oral Med Oral Pathol*. 1977;44(2):306-312. [Crossref]
22. Fluent A. Theory Guide 17.2. Ansys Inc USA. 2016;
23. Haapasalo M, Endal U, Zandi H, Coil J. Eradication of endodontic infection by instrumentation and irrigation solutions. *Endodontic Topics*. 2005;10:77-102. [Crossref]
24. Chow TW. Mechanical effectiveness of root canal irrigation. *J Endod*. 1983;9(11):475-9. [Crossref]
25. Senia ES, Marshall FJ, Rosen S. The solvent action of sodium hypochlorite on pulp tissue of extracted teeth. *Oral Surg Oral Med Oral Pathol*. 1971;31(1):96-103. [Crossref]
26. Guerisoli D, Silva R, Pecora J. Evaluation of some physico-chemical properties of different concentrations of sodium hypochlorite solutions. *Brazilian Endodontic J*. 1998;3:21-23.
27. Gulabivala K, Ng YL, Gilbertson M, Eames I. The fluid mechanics of root canal irrigation. *Physiol Meas*. 2010;31(12):R49-84. [Crossref]
28. Adıgüzel Ö, Gökçen M, Olcay A. Evaluation of the Effect of Needle Tilting Angle on Irrigant Flow in the Root Canal Using Side-Vented Needle by an Unsteady Computational Fluid Dynamics Model The Effect of Needle Tilting Angle on Irrigant Flow. *International Dental Research*. 04/15 2016;6:1-8. [Crossref]
29. McCabe W, Smith J, Harriott P. Unit operations of chemical engineering. 7th edn. ed. 2004.
30. Lambrianidis T, Tosounidou E, Tzoanopoulou M. The effect of maintaining apical patency on periapical extrusion. *J Endod*. 2001;27(11):696-698. [Crossref]
31. Guyton AC, Granger HJ, Taylor AE. Interstitial fluid pressure. *Physiological Rev*. 1971;51(3):527-563. [Crossref]